Rate Equation Model for Nonequilibrium Operating Conditions in a Self-Organized Quantum-Dot Laser

H. Huang and D. G. Deppe, *Fellow, IEEE,*

***Abstract*—A nonequilibrium rate equation model is presented and analyzed for the self-organized quantum dot (QD) laser. The model assumes the QD zero-dimensional levels are coupled to a thermal electron distribution in the wetting layer through reservoir rate equations. By including the energy dependence of the wetting layer reservoir versus temperature, the model accounts for the spectral narrowing of the gain with increasing temperature, the negative temperature coefficient of the lasing threshold, and a reduction of the spectral hole burning with increasing temperature, all found experimentally in QD lasers.**

I. Introduction

SINCE THEIR first demonstration [1], self-organized quantum-dot (QD) lasers have rapidly advanced to become a topic of important research [1]–[21]. Milestones include demonstrations of long-wavelength (1.3 μm) QD lasers on GaAs [5]–[10], QD vertical-cavity surface-emitting lasers (VCSELs) [11]–[16], and 1.3-μm QD VCSELs [17]. Novel fabrication of short cavity edge-emitting QD lasers has also been reported [18]. There is a strong theoretical interest in the physics of the self-organized QD lasers since the zero-dimensional quantum states dramatically alter the laser characteristics from those of the better known planar QW lasers. These differences include the minimum threshold current density [9], [19], the temperature dependence of threshold [6], [21], and spectral hole burning of the optical gain [4], [6], as well as more subtle differences that change the linewidth broadening and chirp. The temperature dependence is particularly interesting, because a negative temperature coefficient can occur over certain temperature ranges [21].

Although there are numerous past theoretical works now published on the operation of QD lasers, few of these are capable of rigorously calculating the negative temperature dependence of the lasing threshold. Self-organized QDs sit "on top of" a wetting layer, so that the QDs' zero-dimensional levels are electronically coupled to the wetting layer's 2-D density of levels. The negative temperature dependence occurs for a range of inhomogeneous broadening, for which quasi-equilibration of the QD ground states with the wetting layer narrows the gain spectrum [21]. Therefore, a theoretical model must be capable of describing both nonequilibrium carrier distributions in the QD zero-dimensional levels at low temperature, as well as a quasi-equilibrium distribution for higher temperature operation. Recently, we presented a rate equation analysis that is capable of accounting for nonequilibrium and quasi-equilibrium carriers within the QDs' zero-dimensional levels [22], [34]. As we show below, these thermal effects in the QD laser can be treated with these rate equations in which the electronic levels are coupled to a Boson reservoir so that the zero-dimensional ground state achieves some steady-state carrier distribution due to carrier relaxation from and thermal escape to the wetting layer of the self-organized QDs. The difference in our present analysis is that the wetting layer is specifically included in the rate equations to globally couple the QDs. Rate equations are sufficient to describe the temperature dependence, since phase information between different quantum states is rapidly destroyed by reservoir coupling. On the other hand, quantum mechanics plays a critical role in determining the correct form of the rate equations, since zero-point fluctuations in the reservoir modes must be included to correctly relate the spontaneous emission, stimulated emission, and absorption rates. In essence, the quantum mechanical coupling of the Boson reservoir leads to the famous Einstein relations between spontaneous emission, stimulated emission, and absorption [23].

Following our earlier work, two other publications also purport to calculate the negative temperature dependence of the QD lasing threshold [24], [25]. Unfortunately, a direct comparison between the equations used below and these papers is not possible, since a mathematical treatment is not given. However, we argue below that the form of the rate equations we present is required to correctly bring any electronic system into equilibrium. Quasi-equilibrium models have also been presented previously that account for the QD laser's increasing threshold current with increasing temperature [26]–[28]. Thermal excitation of charge carriers leads to a greater fraction of these carriers occupying higher energy levels, and the spontaneous light emission that comes from these higher energy levels requires a greater injection current to maintain a fixed population in the QD ground state. In this respect, quasiequilibrium models qualitatively account for the rapidly increasing threshold current above a given temperature, but not the negative temperature coefficient.

The application of the analysis below to multilevel QDs is straightforward, but certainly more tedious. This is carried out simply by additional rate equations for the additional levels. We avoid this complication below, but note that an accurate treatment of the QD laser modulation response, in fact, requires the additional levels because of entropy effects that can arise between the wetting layer and higher energy zero-dimensional levels [29].

Manuscript received October 20, 2000; revised January 31, 2001. This work was supported by the University of New Mexico Opto-Center under the Defence Advanced Research Projects Agency and by the National Science Foundation under Grant ECS9734829.

The authors are with the Microelectronics Research Center, Department of Electrical and Computer Engineering, The University of Texas at Austin, Austin, TX 78712 USA.

Publisher Item Identifier S 0018-9197(01)03488-1.

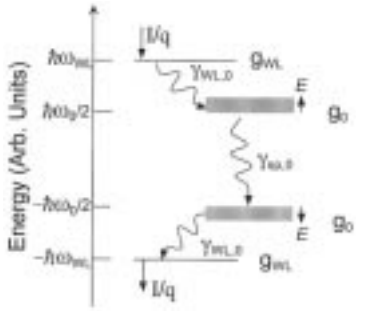

Fig. 1. Schematic illustration of the energy levels of the wetting layer and the ground state. The shaded area illustrates the inhomogeneity of the QD ensemble.

II. Rate Equations

The electron and hole levels of the wetting layer are assumed to be driven by a current source, and the representative energy level diagram illustrated in Fig. 1. Several assumptions are made in order to simplify the analysis and clarify the relevant physics. First, we assume that the wetting layer states contain only low concentrations of electrons and holes. This is typical of most operating conditions of QD lasers, especially for steady-state operation. The wetting layer carriers are then treated using the Boltzmann approximation, as discussed in [26], with the continuum of wetting layer states replaced by an effective density of states. Like [26], we assume that each QD contains only single electron and hole levels (ground state) with a degeneracy of two due to spin. We also assume equal electron and hole relaxation rates.

Using these assumptions, we are able to clearly address the question of how the carrier distribution of a QD ensemble differs from quasiequilibrium, and how this difference can lead to spectral narrowing and threshold reduction with increasing temperature. The wetting layer electron population is given by its degeneracy g_{WL} (related to the density of levels), multiplied by its probability of occupation, taken as $P_{WL,e}$, so that its population is $g_{WL}P_{WL,e}$. The rate equation for the wetting layer electron population is given by [23]

$$\frac{dP_{WL,e}}{dt} = \frac{I}{qg_{WL}} - \gamma_{sp,WL} \cdot \left[P_{WL,e}(1-P_{WL,h}) + \frac{P_{WL,e}-P_{WL,h}}{e^{(E_{WL,e}-E_{WL,h})/(kT)}-1}\right] - \sum_{l=1}^{N_{QD}} g_0\gamma_{WL,0} \cdot \left[P_{WL,e}(1-P_{0,e,l}) + \frac{P_{WL,e}-P_{0,e,l}}{e^{(E_{WL,e}-E_{0,e,l})/(kT)}-1}\right] \quad (1)$$

where

- I current injected into the laser through the wetting layer;
- q electronic charge;
- $P_{WL,h}$ hole population of the wetting layer;
- $\gamma_{sp,WL}$ spontaneous recombination rate coefficient between electrons and holes in the wetting layer;
- $g_0 = 2$ degeneracy of the electron ground state;
- $P_{o,e,l}$ electron population in each of the two zero-dimensional quantum states of a particular QD labeled by l;
- $E_{WL,e} - E_{WL,h}$ energy difference between the wetting layer electron and hole levels;
- $E_{WL,e} - E_{0,e,l}$ energy difference between the wetting layer electron states and a particular QD electron state.

The different energies of the QD ground states, labeled by $E_{0,e,l}$, lead to inhomogeneous broadening. The inclusion of inhomogeneous broadening is the important difference between the present work and [23], which also utilizes nonequilibrium rate equations. The inclusion of stimulated emission and the absorption of phonons is the important difference between the present work and [30], which assumes only spontaneous phonon emission and cannot, therefore, describe thermal effects.

The summation in (1) accounts for electron transfer between the wetting layer states and the zero-dimensional quantum states of the individual QDs. Equation (1) has the form required by quantum mechanics that results in the Einstein relations between spontaneous emission, stimulated emission, and absorption rates that lead to thermal equilibrium and the Fermi distributions for electrons and holes. We assume that the rate coefficient for spontaneous phonon emission $\gamma_{WL,0}$ is independent of the QD energy levels. However, the stimulated phonon emission and absorption rates given by (1) do depend on the QD energy levels through the term $[e^{(E_{WL,e}-E_{0,e,l})/(kT)}-1]^{-1}$.

The electron population of each QD ground state satisfies a rate equation similar to (1). The rate equation is given by

$$\frac{dP_{0,e,l}}{dt} = g_{WL}\gamma_{WL,0} \cdot \left[P_{WL,e}(1-P_{0,e,l}) + \frac{P_{WL,e}-P_{0,e,l}}{e^{(E_{WL,e}-E_{0,e,l})/(kT)}-1}\right] - \gamma_{sp,0} \cdot \left\{P_{0,e,l}(1-P_{0,h,l}) + \left[\beta_l n_L + \frac{1-\beta_l}{e^{(E_{0,e,l}-E_{0,h,l})/(kT)}-1}\right] \cdot (P_{0,e,l}-P_{0,h,l})\right\} \quad (2)$$

where

- $\gamma_{sp,0}$ spontaneous emission rate coefficient between electrons and holes in the QD ground state;
- n_L number of lasing mode photons;
- β_l fraction of spontaneous emission from QD emitter l that couples to the lasing mode.

The lasing mode photon number satisfies the well-known rate equation given by

$$\frac{dn_L}{dt} = -\frac{\omega}{Q}\left[n_L - \frac{1}{e^{\hbar\omega/(kT)}-1}\right] + g_0\gamma_{sp,0}\sum_{l=1}^{N_{QD}}\beta_l \cdot \left\{P_{0,e,l}(1-P_{0,h,l}) + \left[n_L + \frac{1}{e^{(E_{0,e,l}-E_{0,h,l})/(kT)}-1}\right] \cdot (P_{0,e,l}-P_{0,h,l})\right\} \quad (3)$$

where $[e^{\hbar\omega/(kT)}-1]^{-1}$ is the thermal photon number in the lasing mode.

Equations (1)–(3) can be solved with the time derivatives set equal to zero to find the steady-state operating conditions of the QD laser. The differences in the results as compared to a quasiequilibrium approach are interesting. The steady-state electron population in QD l is related to the wetting layer population by (4), shown at the bottom of the page. Under conditions that either the relaxation rate from the wetting layer to the ground state goes to infinity ($\gamma_{WL,0}\rightarrow\infty$), the second term on the right in (4) is negligible, and a quasi-equilibrium distribution is obtained from the first term with

$$P_{WL,e}\approx\frac{\dfrac{P_{0,e,l}}{e^{(E_{WL,e}-E_{0,e,l})/(kT)}-1}}{1-P_{0,e,l}+\dfrac{1}{e^{(E_{WL,e}-E_{0,e,l})/(kT)}-1}}. \tag{5}$$

Equation (5) results in the Fermi distribution for the electron concentration in the wetting layer relative to the QD ground state. Under the approximation that the second term on the right in (4) is negligible, the equations then become the same as quasiequilibrium models [26], [27]. If $P_{0,e,l}=[e^{-(E_{0,e,l}-E_F)/(kT)}+1]^{-1}$ then (5) gives $P_{WL,e}\approx[e^{-(E_{WL,e}-E_F)/(kT)}+1]^{-1}$. However, if the temperature is sufficiently low, the relaxation rate sufficiently slow, or the stimulated emission rate sufficiently large, (4) produces a nonthermal distribution of carriers among the different QDs. Under this other extreme, the electron population in QD l becomes set by (6), shown at the bottom of the page. The current required to support the spontaneous and stimulated light emission must account for the total emission due both to the wetting layer and QDs. The steady-state current is found from (1) to (3) to approximately be

$$\begin{aligned}I=&qg_{WL}\gamma_{sp,WL}\\&\cdot\left[P_{WL,e}(1-P_{WL,h})+\frac{P_{WL,e}-P_{WL,h}}{e^{(E_{WL,e}-E_{WL,h})/(kT)}-1}\right]\\&+qg_0\gamma_{sp,0}\sum_{l=1}^{N_{QD}}\\&\cdot\left\{P_{0,e,l}(1-P_{0,h,l})+\left[\beta_l n_L+\frac{1-\beta_l}{e^{(E_{0,e,l}-E_{0,h,l})/(kT)}-1}\right]\right.\\&\left.\cdot(P_{0,e,l}-P_{0,h,l})\right\}.\end{aligned} \tag{7}$$

The spontaneous coupling of a particular QD l to the lasing mode, given by β_l, depends on QD l's center frequency, its homogeneous linewidth, and its position in the laser cavity [23]. Except in extreme cases, such as when the laser is driven far above threshold, or for small volume, high Q cavities, the polarization of the gain can be assumed to follow the lasing field adiabatically. Under this condition [23], the expression for β_l is found to be

$$\beta_l=\frac{4\pi c^3\hbar^3}{n^3\omega V}\,\frac{\gamma_H/(E_{0,e,l}-E_{0,h,l})}{(E_{0,e,l}-E_{0,h,l}-\hbar\omega)^2+(\hbar\gamma_H)^2}, \tag{8}$$

where

- V volume of the optical mode;
- ω frequency of the lasing mode (or spectral emission);
- c speed of light;
- n refractive index in the cavity;
- $\hbar\gamma_H$ homogeneous energy broadening of the QD (also assumed equal for all QDs).

In QD lasers studied to date, the inhomogeneous broadening due to the different QD sizes results in an approximately Gaussian lineshape for the distribution of $E_{0,e,l}-E_{0,h,l}$ with a full-

$$\begin{aligned}P_{WL,e}=&\frac{\dfrac{P_{0,e,l}}{e^{(E_{WL,e}-E_{0,e,l})/(kT)}-1}}{1-P_{0,e,l}+\dfrac{1}{e^{(E_{WL,e}-E_{0,e,l})/(kT)}-1}}\\&+\frac{\dfrac{\gamma_{sp,0}}{g_{WL}\gamma_{WL,0}}\left\{P_{0,e,l}(1-P_{0,h,l})+\left[\beta_l n_L+\dfrac{1-\beta_l}{e^{(E_{0,e,l}-E_{0,h,l})/(kT)}-1}\right](P_{0,e,l}-P_{0,h,l})\right\}}{1-P_{0,e,l}+\dfrac{1}{e^{(E_{WL,e}-E_{0,e,l})/(kT)}-1}}\end{aligned} \tag{4}$$

$$P_{WL,e}\approx\frac{\dfrac{\gamma_{sp,0}}{g_{WL}\gamma_{WL,0}}\left\{P_{0,e,l}(1-P_{0,h,l})+\left[\beta_l n_L+\dfrac{1-\beta_l}{e^{(E_{0,e,l}-E_{0,h,l})/(kT)}-1}\right](P_{0,e,l}-P_{0,h,l})\right\}}{1-P_{0,e,l}.} \tag{6}$$

width-at-half-maximum (FWHM) that greatly exceeds the homogenous FWHM given by $\hbar\gamma_H$. Spectral hole burning can then be observed, with the result of highly multimode laser operation [4]. Note that this is predicted by the nonequilibrium steady-state expression (4) when β_l varies significantly for different QDs, and the photon number is sufficiently large so that the second term in (4) dominates and approximately becomes (6).

The spontaneous spectrum is proportional to $P_{0,e,l}(1 - P_{0,h,l})$, which is nearly independent of $E_{0,e,l} - E_{0,h,l}$ for low temperature but becomes dependent on this energy difference at higher temperatures. The dependence at higher temperatures is due to the larger rate of thermal excitation out of the QDs for larger $E_{0,e,l} - E_{0,h,l}$. The gain spectrum is proportional to

$$\sum_{l=1}^{N_{QD}} \frac{\gamma_H/(E_{0,e,l} - E_{0,h,l})}{(E_{0,e,l} - E_{0,h,l} - \hbar\omega)^2 + (\hbar\gamma_H)^2} \frac{P_{0,e,l} - P_{0,h,l}}{\omega}$$

where ω is the frequency of interest in the gain spectrum. Again thermal effects come into the gain spectrum due to the temperature dependence of the population $P_{0,e,l} - P_{0,h,l}$ for QDs with different photon emission energies, $E_{0,e,l} - E_{0,h,l}$.

Debate exists in the literature as to the cause for the reduction in the number of lasing modes with increasing temperature. Although it has been suggested that quasiequilibration through the wetting layer leads to the reduction of the number of lasing modes [6], it has also been argued that such spectral narrowing can only be explained by an increase in the homogeneous linewidth, $\hbar\gamma_H$ [31]–[33]. The calculations below show that even with an unchanging homogeneous linewidth, quasiequilibration of the QD ensemble's ground state with the wetting layer decreases the population inversion across the entire gain spectrum. Because of this reduction, the number of modes brought above threshold once one mode lases will also be decreased, thus reducing the total measured spectral width of lasing modes. Therefore, either quasiequilibration of the QD ensemble or an increase in the homogeneous linewidth can reduce the total spectral width of the QD laser with increasing temperature. More detailed calculations than those presented here are required to determine the true contributions from either mechanism.

III. Calculated Results

The steady-state solutions to the rate equations given above are used to calculate the population characteristics, and thus the gain characteristics, of a QD ensemble. Although, in general, we should consider that the electrons and holes have different electronic structures and different relaxation rates, the assumption of a symmetrical electronic structure and equal relaxation rates for electrons and holes results in $P_{0,e} = P_{0,h}$ and this considerably simplifies the calculations. While this assumption greatly simplifies the math and discussion, it still fully illustrates the importance of the nonequilibrium rate equation approach in calculating key features of QD lasers that are found experimentally.

The characteristics of 1.3-μm QD emitters are now fairly well-known, and to illustrate the nonequilibrium approach, we use their parameter values for the inhomogeneous broadening, QD density, and spontaneous decay rates (or dipole strengths) to calculate the light emission characteristics for QD lasers from the equations given above. These QDs have a density of 1.5×10^{10} cm^{-2}, spontaneous decay rate of 2.5×10^9 s^{-1}, and a Gaussian full-width-at-half-maximum of 30 meV [23]. For laser characteristics, we consider a QD edge-emitter with cavity length of 3 mm and stripe width of 10 μm. As for the relaxation rate and the degeneracy of the wetting layer, we choose $\gamma_{WL,0} = 2.5 \times 10^{12}/(N_{QD} \cdot g_0)$ sec^{-1} and $g_{WL} = 40N_{QD} \cdot g_0$. The cavity length is chosen so that the threshold occurs at ~40% of the maximum gain. The average energy difference between the wetting layer and QD electron (and hole) levels, $\Delta E_{WL,0}$, is varied in some of the calculations to determine how this energy influences the QD laser's temperature dependence.

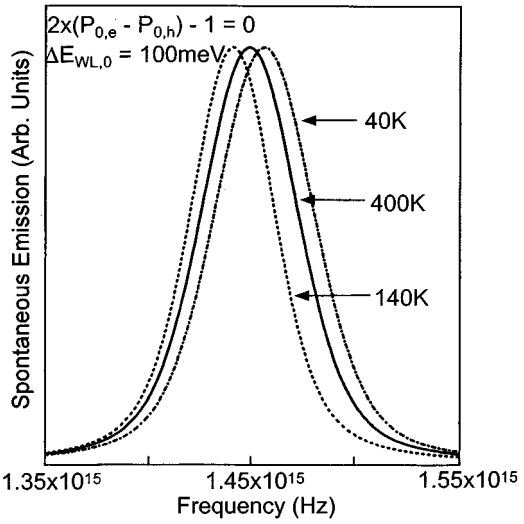

Fig. 2. Spontaneous emission spectrum at transparency for three different temperatures of 40, 140, and 400 K. The energy separation between the wetting layer and the ground state is 100 meV.

Fig. 2 shows how the spontaneous emission spectrum changes for different temperatures as predicted by the rate equations presented in Section II. Consistent with most experimental results, the shape of the spontaneous spectrum is only weakly dependent on temperature. A small red-shift in the peak emission frequency occurs with increasing temperature. This red-shift is due to a stronger thermal excitation out of the QDs into the wetting layer for those QDs with higher energy emission. This stronger thermal excitation out of the QDs decreases the electron occupation of the higher energy QDs and increases the electron occupation of the lower energy QDs.

Fig. 3 shows calculated plots of the FWHM for different $\Delta E_{WL,0}$ when the average population inversion is at transparency $2x(P_{0,e} - P_{0,h}) - 1 = 0$. Fig. 3 shows that the FWHM is quite temperature dependent for an energy separation from the wetting layer of $\Delta E_{WL,0} = 100$ meV, versus the larger energy separations of 250 or 400 meV. At low temperature (~50 K), the FWHM is due to the inhomogeneous broadening of the QD energy levels. As the temperature is increased, the FWHM decreases significantly to ~33 meV at ~150 K, and this decrease is due to thermal excitation of the carriers out

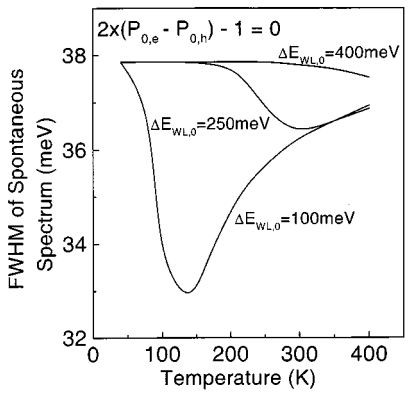

Fig. 3. FWHM of the spontaneous spectrum versus temperature at transparency. The energy separations are 100, 250, and 400 meV.

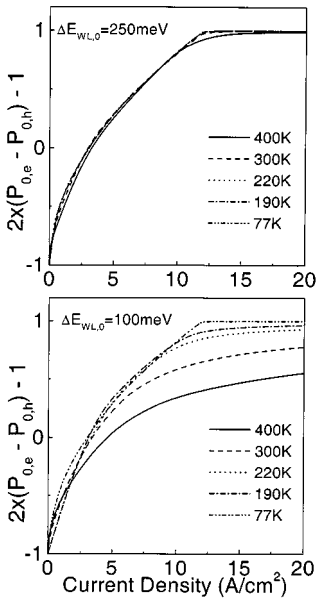

Fig. 4. Ground-state population inversion versus current density for various temperatures. The energy separations are 100 and 250 meV.

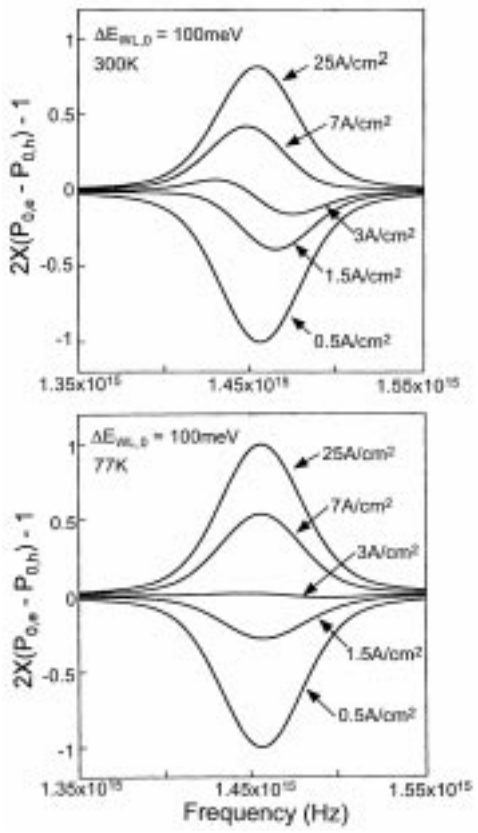

Fig. 5. Ground-state population inversion versus frequency for two different temperatures of 77 and 300 K. The injected current density is varied while the energy separation is kept fixed at 100 meV.

of the QDs with larger electron-hole energy separations. As the temperature is increased further yet, the FWHM increases again due to thermal broadening. These same features have been measured experimentally [28]. For the larger $\Delta E_{WL,0}$, the temperature dependence of the FWHM is less dramatic, since the temperature at which thermal excitation out of the higher energy QDs is closer to the temperature at which thermal broadening competes with the inhomogeneous broadening. To our knowledge, the rate equation approach presented in Section II is the first analysis of QD lasers to capture the spontaneous linewidth dependence on temperature found experimentally [28].

Fig. 4 shows the temperature dependence of the peak population inversion on current density for five different temperatures, and two different energy separations $\Delta E_{WL,0}$. Similar calculations have been presented by Park *et al.* [28]. The smaller energy separation of $\Delta E_{WL,0} = 100$ versus 250 meV increases the temperature dependence of inversion, as is described in earlier papers by Asryan and Suris [26].

Fig. 5 shows the calculated inversion spectra, proportional to the gain spectra, for different current densities for two different temperatures, 77 and 300 K, for $\Delta E_{WL,0} = 100$ meV. Again, to our knowledge, this represents the first report of the calculated temperature dependence of the inversion spectrum, made possible with the rate equation approach in Section II. At 77 K, the gain spectra are nearly symmetrical with the Gaussian shape of the inhomogeneously broadened QD ensemble. At 300 K, however, the temperature dependence of the population inversion creates an asymmetrical gain spectrum, and near transparency the population inversion for lower frequencies may be greater than zero, while at higher frequencies, the population inversion may be less than zero. This asymmetry is directly attributable to the larger thermalization rate out of higher energy QDs of the ensemble.

The thermalization of carriers from the higher energy QDs that leads to the asymmetrical gain spectra as shown in Fig. 5 increases the optical gain from the lower energy QDs for the same bias current. The rearrangement of the carrier distribution leads to the novel behavior that the threshold current density can, in fact, decrease with increasing temperature for a QD laser, and thus show a negative characteristic temperature coefficient. This negative temperature coefficient is illustrated by Fig. 6, in which the current density required to reach a specific population inversion at the peak of the spectral inversion curve is plotted versus temperature. Three values of peak population inversion are included: 0 (transparency), 0.25 of the maximum inversion, and

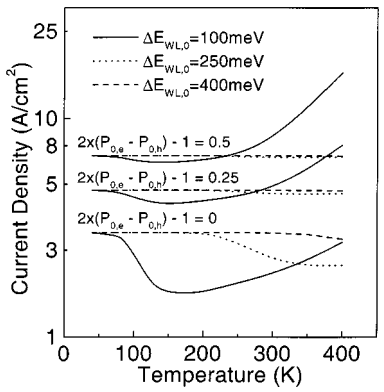

Fig. 6. Current density versus temperature at three different energy separations of 100, 250, and 400 meV. The peak ground state population is varied from 0, to 0.25, and to 0.5, of the maximum value. The current density is in log scale.

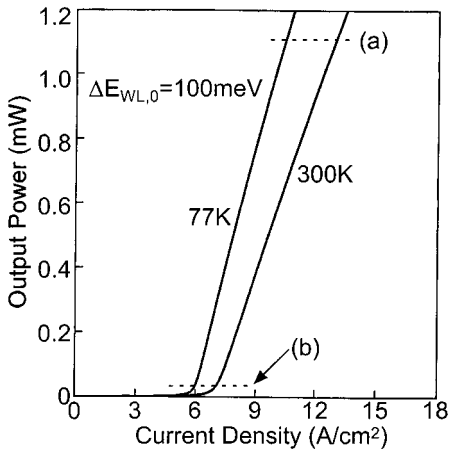

Fig. 7. Light versus current curve at two different temperatures of 77 and 300 K. Here, the energy separation is 100 meV. The dashed lines indicate the two chosen output powers to see the spectral hole burning effect.

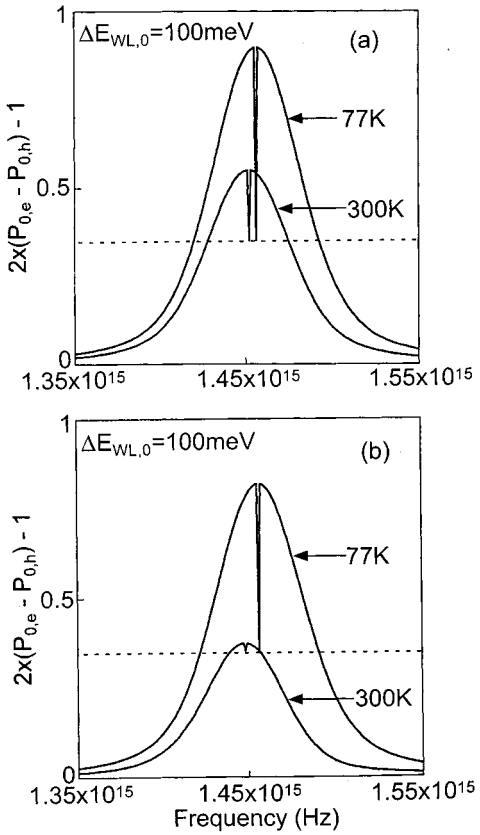

Fig. 8. Ground-state population inversion versus frequency for two different temperatures of 77 nd 300 K. The energy separation is fixed at 100 meV. The dashed line indicates the cavity loss rate. Here, (a) and (b) correspond to the two output powers chosen from Fig. 7.

0.5 of the maximum inversion, each for three different values of $\Delta E_{WL,0}$. For each case, we find that the required current density, in fact, decreases with increasing temperature. The most dramatic decrease is for transparency when $\Delta E_{WL,0}$ is smaller, because the spectral asymmetry in the population inversion is largest near transparency and the smaller $\Delta E_{WL,0}$ leads to a stronger thermalization behavior for the QD ensemble through the wetting layer. In all cases, the decreasing current density required for a given population inversion predicts a negative temperature coefficient for the lasing threshold in the same temperature regime. Also consistent with Asryan and Suris, a larger $\Delta E_{WL,0}$ leads to a significantly reduced temperature dependence for the QD laser's threshold current density.

Finally, we examine the predictive power of the nonequilibrium rate equation approach in describing the gain saturation for QD lasers above threshold. Because of the zero-dimensional energy levels and inhomogeneous broadening, QD lasers can show dramatic spectral hole burning that is not observed in planar QW lasers [4]. Typically, whether spectral hole burning occurs or not is attributed to whether the gain region is homogeneously or inhomogeneously broadened, and the significant decrease in spectral hole burning has been reported as due to an increase in the homogeneous linewidth caused by an increase in dipole dephasing of the QDs [31]–[33]. Here, we show that increased dipole dephasing, and thus an increase in the QD homogeneous linewidth, is not a requirement for the decrease in spectral hole burning with increasing temperature, and that quasiequilibration with the wetting layer will also decrease the observed degree of spectral hole burning.

Fig. 7 shows 77- and 300-K calculated light versus current curves from the equations presented in Section II. As above, the calculated results show the general trends for QD lasers. The increasing photon number above lasing threshold increases the importance of the second term on the right of (4). Because the spontaneous coupling factor depends on the QD's homogeneous linewidth, as given by (8), it seems reasonable to expect that a spectral hole of the same width will be burned in the optical gain by the spectrally sharp lasing mode [32], [33]. Despite this, it is also the case that the QDs can separately equilibrate with the wetting layer. For true quasiequilibration with the wetting layer, clamping of the optical gain in one spectral region of the QD ensemble would then result in population clamping of all QDs, independent of whether they contribute to stimulated emission in the lasing mode.

Fig. 8 demonstrates this effect using the rate equation approach of Section II. The two curves shown in Fig. 8(a) are the population inversions calculated for the same output power of the laser but at two different temperatures, 77 and 300 K, with $\Delta E_{WL,0} = 100$ meV. The homogeneous linewidth is taken

as the same for both curves and much less than the inhomogeneous linewidth, and we have assumed that only one mode lases in each case, such as for a distributed feedback laser, to clearly illustrate the different population inversion behavior for the two different temperatures. For both temperatures, the population inversion clamps at precisely the same value needed to achieve threshold for that frequency at the peak of the respective optical gains. However, the amount by which the population grows at nonlasing frequencies is dramatically different for the two different temperatures. Fig. 8(a) clearly shows that the spectral width of the population inversion that can rise above the threshold value is different for the two different temperatures. For a multimode Fabry–Perot laser, we expect the effect to be more dramatic, since every mode that approaches threshold will further suppress the population inversion across the entire spectral width of the QD ensemble. Fig. 8(b) shows the similar effect but close to threshold.

This effect, due to thermalization of electrons and holes into the wetting layer—as opposed to an increase of the homogeneous linewidth—is consistent with experimental results, showing that QD lasers become more single mode for the same temperatures at which negative temperature coefficients for the lasing threshold are observed [6], [21], [23]. Both effects are due to quasiequilibration. These results show that both quasiequilibration and an increase in the homogeneous linewidth must be considered when analyzing the lasing spectrum changes in multimode QD lasers.

IV. Summary

A nonequilibrium rate equation approach is used to analyze QD light emission and laser characteristics. The rate equations used to describe relaxation and thermal escape from the QDs are consistent with Einstein treatment of coupling electronic levels to a Boson reservoir. Because of this, these rate equations capture several experimental phenomenon found in QD lasers, but not previously found in the calculated results of other QD laser models. These are the narrowing and increase of the spontaneous linewidth with increasing temperature, the asymmetry of the gain spectrum that develops with increasing temperature and that produces a negative temperature coefficient for the lasing threshold, and the suppression of the entire gain spectrum due to lasing at one frequency, despite a narrow homogenous linewidth in the individual QDs.

The limitation in our present paper is the idealistic treatment of the electronic structure and scattering rates assumed to be equal for electrons and holes. However, this assumption is not fundamental to the nonequilibrium rate equation approach, and the same approach as presented above that uses more accurate QD parameters and electronic structures will have important predictive capabilities for modeling QD lasers.

References

[1] N. Kirstaedter, N. N. Ledentsov, M. Grundmann, D. Bimberg, V. M. Ustinov, S. S. Ruvimov, M. V. Maximov, P. S. Kop'ev, Z. I. Alferov, U. Richter, P. Werner, U. Gosele, and J. Heydenreich, "Low threshold, large T_0 injection laser emission from InGaAs quantum dots," *Electron. Lett.*, vol. 30, pp. 1416–1417, 1994.

[2] H. Shoji, K. Mukai, N. Ohtsuka, M. Sugawara, T. Uchida, and H. Ishikawa, "Lasing at three-dimensionally quantum-confined sublevel of self-organized $In_{0.5}Ga_{0.5}As$ quantum dots by current injection," *IEEE Photon. Technol. Lett.*, vol. 7, pp. 1385–1387, 1995.

[3] K. Kamath, P. Bhattacharya, T. Sosnowski, T. Norris, and J. Phillips, "Room-temperature operation of $In_{0.4}Ga_{0.6}As$ self-organized quantum dot lasers," *Electron. Lett.*, vol. 32, pp. 1374–1375, 1996.

[4] Q. Xie, A. Kalburge, P. Chen, and A. Madhukar, "Observation of lasing from vertically self-organized InAs three-dimensional island quantum boxes on GaAs (001)," *IEEE Photon. Technol. Lett.*, vol. 8, pp. 965–967, 1996.

[5] D. L. Huffaker, G. Park, Z. Zou, O. B. Shchekin, and D. G. Deppe, "1.3 μm room-temperature GaAs-based quantum-dot laser," *Appl. Phys. Lett.*, vol. 73, pp. 2564–2466, 1998.

[6] G. Park, D. L. Huffaker, Z. Zou, O. B. Shchekin, and D. G. Deppe, "Temperature dependence of lasing characteristics for long-wavelength (1.3 μm) GaAs-based quantum dot lasers," *IEEE Photon. Technol. Lett.*, vol. 11, pp. 301–303, 1999.

[7] S. Mukai, N. Ohtsuka, H. Shoji, M. Sugawara, N. Yokoyama, and H. Ishikawa, "1.3 μm CW lasing of InGaAs/GaAs quantum dots at room temperature with a threshold current of 8 mA," *IEEE Photon. Technol. Lett.*, vol. 11, pp. 1205–1207, 1999.

[8] G. Park, O. B. Shchekin, S. Csutak, and D. G. Deppe, "Room-temperature continuous-wave operation of a single-layered 1.3 μm quantum dot laser," *Appl. Phys. Lett.*, vol. 75, pp. 3267–3269, 1999.

[9] G. Park, O. B. Shchekin, D. L. Huffaker, and D. G. Deppe, "Low threshold oxide-confined 1.3 μm quantum dot laser," *IEEE Photon. Technol. Lett.*, vol. 12, pp. 230–232, 2000.

[10] Y. M. Shernyakov, D. A. Bedarev, E. Y. Kondrat'eva, P. S. Kop'ev, A. R. Kovsh, N. A. Maleev, M. V. Maximov, S. S. Mikhrin, A. F. Tsatsul'nikov, V. M. Ustinov, B. V. Volovik, A. E. Zhukov, Z. I. Alferov, N. N. Ledentsov, and D. Bimberg, "1.3 μm GaAs-based laser using quantum dots obtained by activated spinodal decomposition," *Electron. Lett.*, vol. 35, pp. 898–900, 1999.

[11] H. Saito, K. Nishi, I. Ogura, S. Sugov, and Y. Sugimoto, "Room temperature lasing operation of a quantum dot vertical cavity surface emitting laser," *Appl. Phys. Lett.*, vol. 69, pp. 3140–3142, 1996.

[12] D. L. Huffaker, O. Baklenov, L. A. Graham, B. G. Streetman, and D. G. Deppe, "Quantum dot vertical-cavity surface-emitting laser with a dielectric aperture," *Appl. Phys. Lett.*, vol. 70, pp. 2356–2358, 1997.

[13] D. L. Huffaker, L. A. Graham, and D. G. Deppe, "Low-threshold continuous-wave operation of an oxide-confined vertical-cavity surface-emitting laser based on a quantum dot active region and half-wave cavity," *Electron. Lett.*, vol. 33, pp. 1225–1226, 1997.

[14] J. A. Lott, N. N. Ledentsov, V. M. Ustinov, A. Y. Egorov, A. E. Zhukov, P. S. Kop'ev, Z. I. Alferov, and D. Bimberg, "Vertical-cavity lasers based on vertically coupled quantum dots," *Electron. Lett.*, vol. 33, pp. 1150–1151, 1997.

[15] D. L. Huffaker, H. Deng, and D. G. Deppe, "1.15 μm wavelength oxide-confined quantum dot vertical-cavity surface-emitting laser," *IEEE Photon. Technol. Lett.*, vol. 10, pp. 185–187, 1998.

[16] Z. Zou, D. L. Huffaker, S. Csutak, and D. G. Deppe, "Ground state lasing from a quantum dot oxide-confined vertical-cavity surface-emitting laser," *Appl. Phys. Lett.*, vol. 75, pp. 22–25, 1999.

[17] J. A. Lott, N. N. Ledentsov, V. M. Ustinov, N. A. Maleev, A. E. Zhukov, A. R. Kovsh, M. V. Maximov, B. V. Volovik, Z. I. Alferov, and D. Bimberg, "InAs–InGaAs quantum dot VCSEL's on GaAs substrates emitting at 1.3 μm," *Electron. Lett.*, vol. 36, pp. 1384–1385, 2000.

[18] S. Rennon, K. Avary, F. Klopf, A. Wolf, M. Emmerling, J. P. Reithmaier, and A. Forchel, "Quantum dot microlasers," *Electron. Lett.*, vol. 36, pp. 1548–1550, 2000.

[19] G. T. Liu, A. Stintz, H. Li, K. J. Malloy, and L. F. Lester, "Extremely low room-temperature threshold current density diode lasers using InAs dots in InGaAs quantum well," *Electron. Lett.*, vol. 35, pp. 1163–1165, 1999.

[20] L. Harris, D. J. Mowbray, M. S. Skolnic, M. Hopkinson, and G. Hill, "Emission spectra and mode structure of InAs/GaAs self-organized quantum dot lasers," *Appl. Phys. Lett.*, vol. 73, pp. 969–971, 1998.

[21] A. E. Zhukov, V. M. Ustinov, A. Y. Egorov, A. R. Kovsh, A. F. Tsatsulnikov, N. N. Ledentsov, S. V. Zaitsev, N. Y. Gordeev, P. S. Kopev, and Z. I. Alferov, "Negative characteristic temperature of InGaAs quantum dot injection laser," *Jpn. J. Appl. Phys.*, vol. 36, pp. 4216–4218, 1997.

[22] P. L. Knight and L. Allen, *Concepts of Quantum Optics*. Oxford, U.K.: Pergamon, 1983, pp. 93–104.

[23] D. G. Deppe, D. L. Huffaker, S. Csutak, Z. Zou, G. Park, and O. B. Shchekin, "Spontaneous emission and threshold characteristics of 1.3 μm InGaAs–GaAs quantum dot GaAs-based lasers," *IEEE J. Quantum Electron.*, vol. 35, pp. 1502–1508, 1999.

[24] M. Grundmann, O. Stier, S. Bognar, C. Ribbat, F. Heinrichsdorff, and D. Bimberg, "Optical properties of self-organized quantum dots: Modeling and experiments," *Phys. Stat. Sol. (a)*, vol. 178, pp. 255–262, 2000.
[25] M. Grundmann, "The present status of quantum dot lasers," *Phys. E*, vol. 5, pp. 167–184, 2000.
[26] L. V. Asryan and R. A. Suris, "Temperature dependence of the threshold current density of a quantum dot laser," *IEEE J. Quantum Electron.*, vol. 34, pp. 841–850, 1998.
[27] ——, "Inhomogeneous line broadening and the threshold current density of a semiconductor quantum dot laser," *Semicond. Sci. Tech.*, vol. 11, pp. 554–567, 1996.
[28] G. Park, O. B. Shchekin, and D. G. Deppe, "Temperature dependence of gain saturation in multi-level quantum dot lasers," *IEEE J. Quantum Electron.*, vol. 36, pp. 1065–1071, 2000.
[29] D. G. Deppe and D. L. Huffaker, "Quantum dimensionality, entropy, and the modulation response of quantum dot lasers," *Appl. Phys. Lett.*, vol. 77, pp. 3325–3327, 2000.
[30] M. Grundmann and D. Bimberg, "Theory of random population for quantum dots," *Phys. Rev. B*, vol. 55, pp. 9740–9745, 1997.
[31] Y. Nambu, A. Tomita, H. Saito, and K. Nishi, "Effects of spectral broadening and cross relaxation on the gain saturation characteristics of quantum dot laser amplifiers," *Jpn. J. Appl. Phys.*, vol. 38, pp. 5087–2095, 1999.
[32] A. Sakamoto and M. Sugawara, "Theoretical calculation of lasing spectra of quantum dot lasers; effect of homogeneous broadening of optical gain," *IEEE Photon. Technol. Lett.*, vol. 12, pp. 107–109, 2000.
[33] M. Sugawara, K. Mukai, Y. Nakata, H. Ishikawa, and A. Sakamoto, "Effect of homogenous broadening of optical gain on lasing spectra in self-assembled InGaAs/GaAs quantum dot lasers," *Phys. Rev. B*, vol. 61, pp. 7595–7603, 2000.
[34] A. Einstein, "On the quantum theory of radiation," *Phys. Z.*, vol. 18, p. 121, 1917.

H. Huang was born in Shanghai, China, in 1970. He received the B.S. degree from Fudan University in 1991 and the M.S. degree from Cal State Fullerton in 1998, both in physics, and is currently working toward the Ph.D. degree in electrical engineering at the University of Texas at Austin.

His research interests include microcavity physics, edge emitters, and VCSELs.

D. G. Deppe (S'85–M'90–SM'97–F'00) received the B.S., M.S., and Ph.D. degrees in electrical engineering from the University of Illinois at Champaign-Urbana, where his thesis work centered around atom diffusion processes in III-V semiconductor heterostructures and semiconductor laser fabrication and characterization.

He was with Hewlett-Packard from 1982 to 1984, working on Si integrated circuits. From 1988 to 1990, he was a Member of Technical Staff at AT&T Bell Laboratories, Murray Hill, NJ, researching semiconductor lasers. He is presently a Professor in the Electrical and Computer Engineering Department, University of Texas at Austin, where he holds the Robert and Jane Mitchell Endowed Faculty Fellowship in Engineering. His research specialties include III-V semiconductor device fabrication, optoelectronics, and laser physics. He has published over 150 technical journal articles, authored or co-authored over 100 conference papers with many invited presentations, and holds six U.S. patents with three additional pending.

Dr. Deppe received the Nicholas Holonyak Jr. Award from the Optical Society of America (OSA) for the development of the oxide-confined VCSEL and the National Science Foundation Presidential Young Investigator and the Office of Naval Research Young Investigator Awards. He is a Fellow of the OSA.